



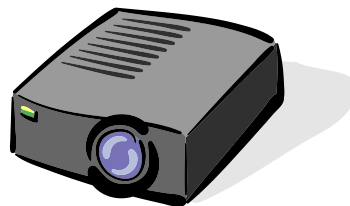
# Electrical Capacitance Volume Tomography: An Imaging Tool for Multiphase Flow Systems

Qussai Marashdeh<sup>1,2</sup>, Fei Wang<sup>2</sup>, and L.S. Fan<sup>2</sup>

<sup>1</sup>Tech4Imaging LLC

<sup>2</sup>The Ohio State University

Department of Chemical and Biomolecular Engineering



# Introduction

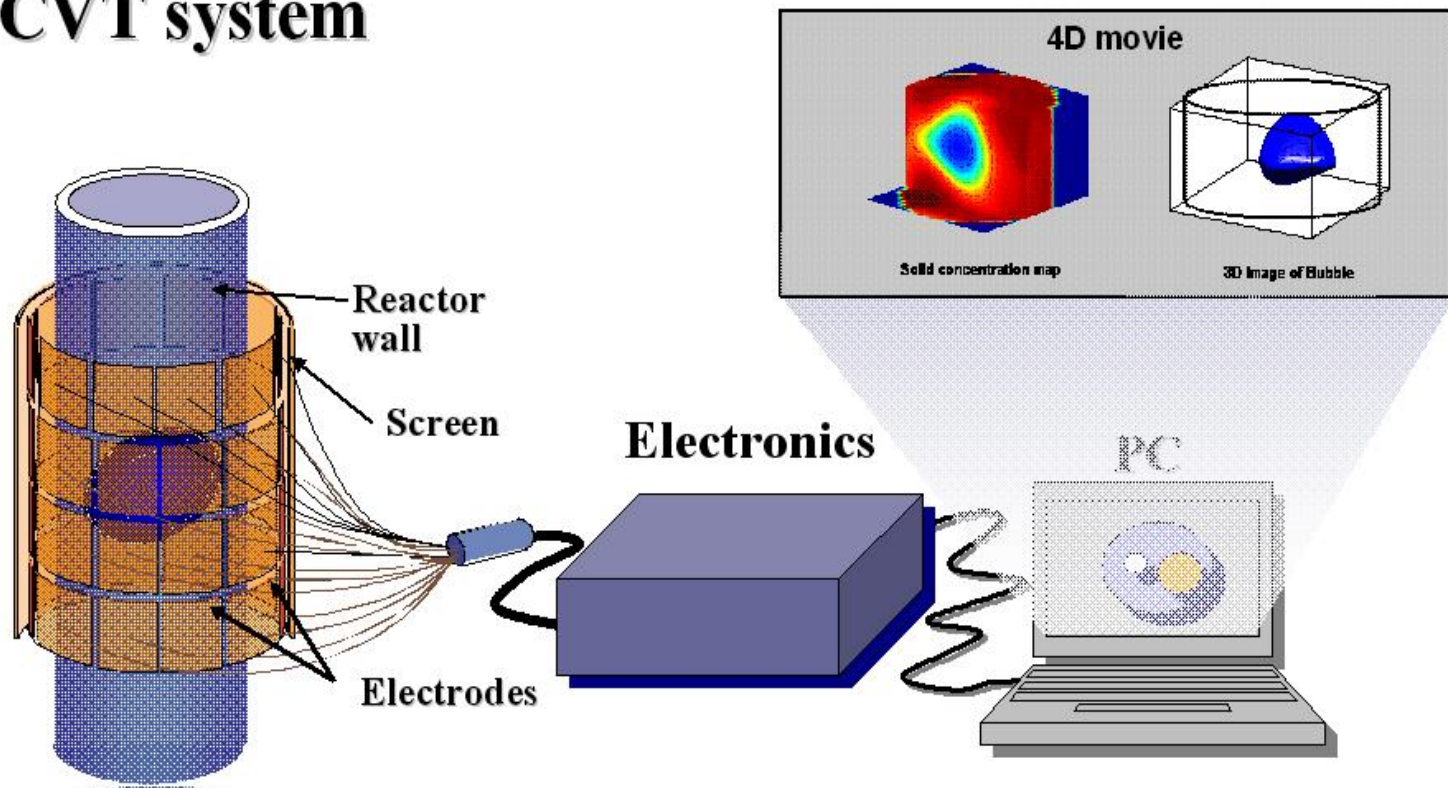
- ◆ Electrical Capacitance Volume Tomography (ECVT) is a 3D imaging technique for viewing cold flow processes. It can potentially be applied to hot units too.
- ◆ ECVT is among few known non-invasive imaging tools that can be used for commercial applications (low cost, suitable for scale-up, fast, and safe)
- ◆ Tech4Imaging LLC is a spin-off company from The Ohio State University to develop and commercialize imaging technologies, including ECVT.
- ◆ Tech4Imaging, with DOE support, is developing a complete system of acquisition hardware, sensors, and reconstruction software for.

# Preface

1. ECVT Technology
2. Verification
3. Jet Example
4. Velocimetry
5. Sensors and Scale up Application
6. Complex geometries

# ECVT System

## ECVT system

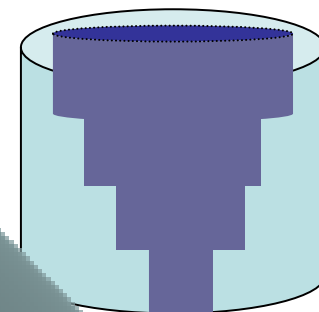
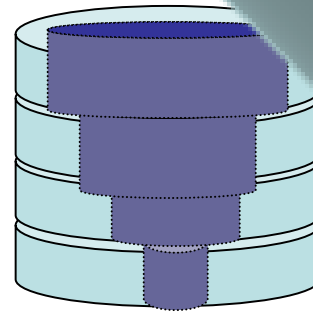


# Volume Tomography Concept

## Conventional Tomography

2D  
Reconstruction

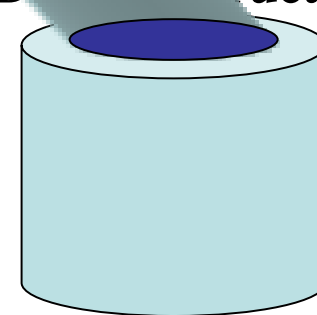
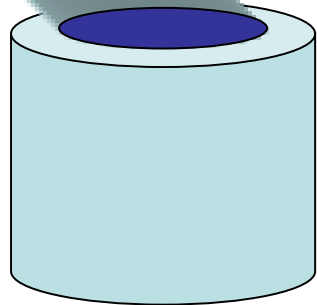
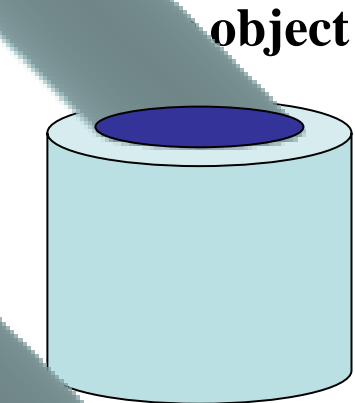
Static 3D  
Reconstruction



## Volume-Tomography

Volume (3D)  
Image Reconstruction

Dynamic  
3D Reconstruction



# ECVT technique

Reconstruction	Methodology	Characteristics	Example
Single Step Linear Back Projection	The sensor system is linearized (usually by constructing a sensitivity matrix). The image is obtained by back projecting the capacitance vector using the sensitivity matrix.	Fast, low image resolution, and introducing image artifacts	LBP
Iterative Linear Back Projection	The mean square error between the capacitance data and forward solution of the final image is minimized by iterative linear projections using the sensitivity matrix.	Slower than Single Step Linear. Providing better images than Single Step	Landweber ILBP
Optimization	A set of objective functions are minimized iteratively to provide the most likely image. Different optimization algorithms and objective functions can be used.	Slower than Iterative Linear Back Projection. Providing better images than Iterative Linear Back Projection	3D-NNMOIRT

# 3D-NNMOIRT

## Objective functions

**Negative entropy function**  $f_1(\mathbf{G}) = \gamma_1 \sum_{j=1}^N G_j \ln G_j$

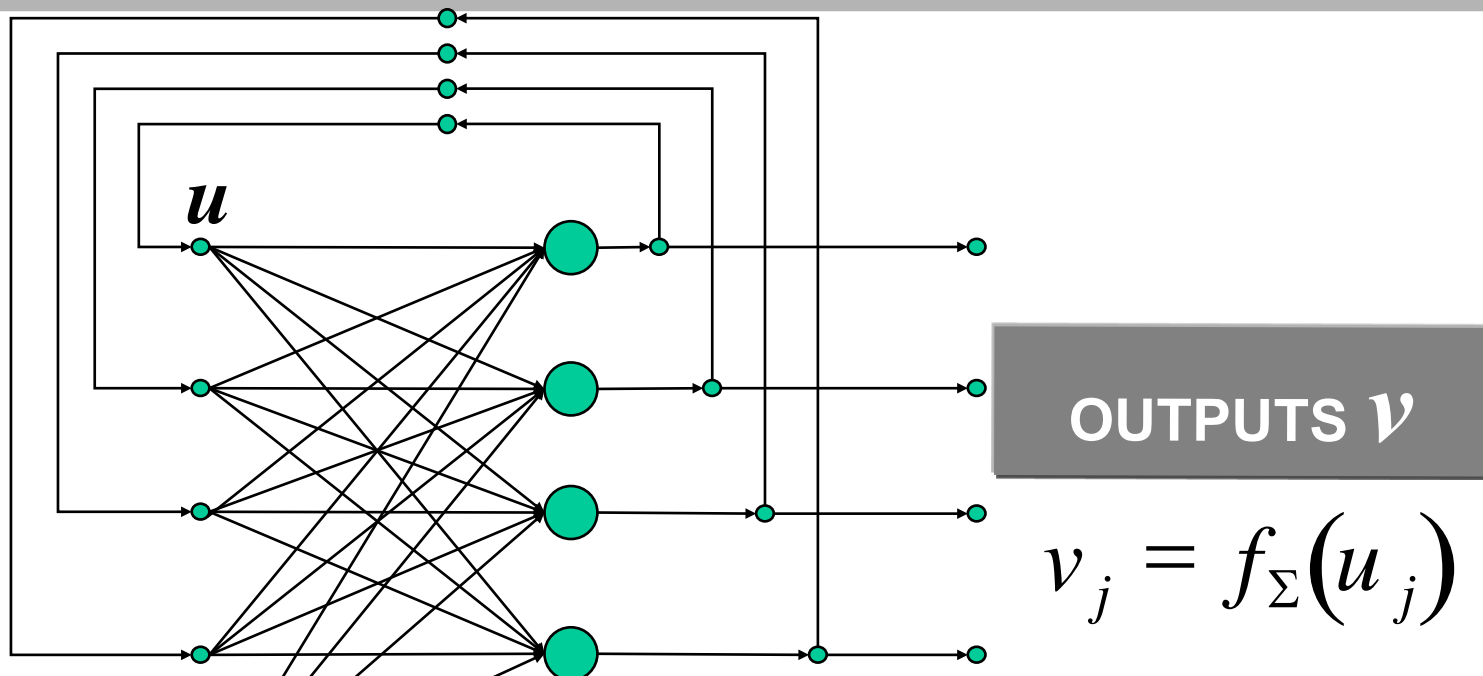
**Error function**  $f_2(\mathbf{G}) = \frac{1}{2} \gamma_2 \|\mathbf{S}\mathbf{G} - \mathbf{C}\|^2 = \gamma_2 \sum_{i=1}^M \left( \sum_{j=1}^N S_{ij} G_j - C_i \right)^2$

**3-D Smoothness function**  $f_3(\mathbf{G}) = \frac{1}{2} \gamma_3 (\mathbf{G}^T \mathbf{X} \mathbf{G} + \mathbf{G}^T \mathbf{G})$

**3-to-2D and 3-to-1D matching function for 3-D imaging**

$$\begin{aligned} f_4(\mathbf{G}) &= \frac{1}{2} \gamma_4 \left\{ \left\| \mathbf{H}^1 \mathbf{G} - \mathbf{G}_{2D}^1 \right\|^2 + \left\| \mathbf{H}^2 \mathbf{G} - \mathbf{G}_{2D}^2 \right\|^2 \right\} \\ &= \frac{1}{2} \gamma_4 \left\{ \sum_{j=1}^{N_{1D}} \left( \sum_{k=1}^N H_{jk}^1 G_k - G_{1D,j} \right)^2 + \sum_{j=1}^{N_{2D}} \left( \sum_{k=1}^N H_{jk}^2 G_k - G_{2D,j} \right)^2 \right\} \end{aligned}$$

# Hopfield Network



INPUTS  
(Initial conditions)

OUTPUTS  $v$

$$v_j = f_{\Sigma}(u_j)$$

$$C_{0j} \frac{du_j}{dt} = - \frac{\partial E(\mathbf{v})}{\partial v_j}$$

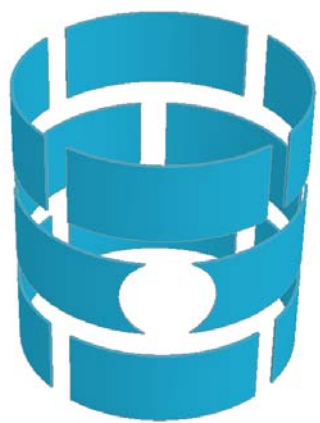
$$\begin{aligned} \frac{dE(\mathbf{v})}{dt} &= \sum_{j=1}^N \frac{\partial E(\mathbf{v})}{\partial v_j} \frac{dv_j}{dt} = - \sum_{j=1}^N C_{0j} \frac{du_j}{dt} \frac{dv_j}{dt} \\ &= - \sum_{j=1}^N C_{0j} \left[ \frac{\partial f_{\Sigma}(u_j)}{\partial u_j} \right] \left( \frac{du_j}{dt} \right)^2 = - \sum_{j=1}^N C_{0j} \left[ \frac{\partial f_{\Sigma}^{-1}(v_j)}{\partial v_j} \right] \left( \frac{dv_j}{dt} \right)^2 \end{aligned}$$

$$\frac{dE}{dt} \leq 0; \frac{du_j}{dt} = \frac{dv_j}{dt} = 0, t \rightarrow \infty$$



## 2. ECVT Verification

- 1) Comparison of the local time-averaged solids concentrations by **ECVT**, **ECT**, and **optical fiber probe**
- 2) Comparison of the time-averaged cross-sectional solids concentrations by **ECT** and **optical fiber probe** and the time-averaged volume solids concentration obtained by **ECVT** and **pressure transducer**
- 3) Comparison of **ECVT** and **MRI**



## ECVT measurement

Outlet air

Cyclone

Column

ECVT sensors

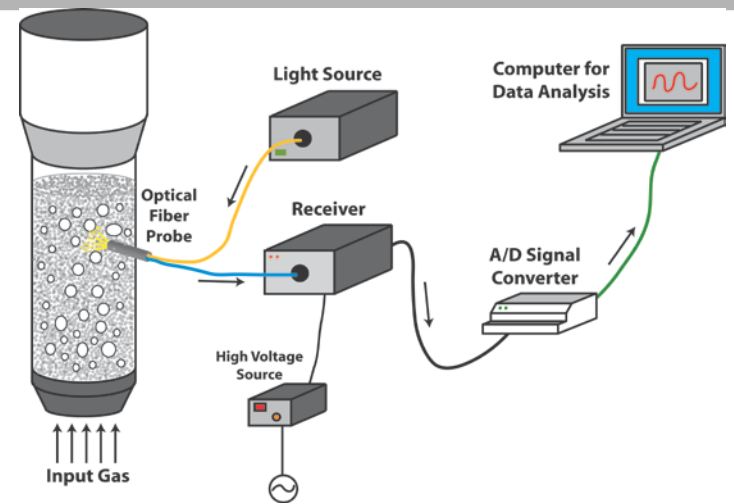
Distributor

Inlet air

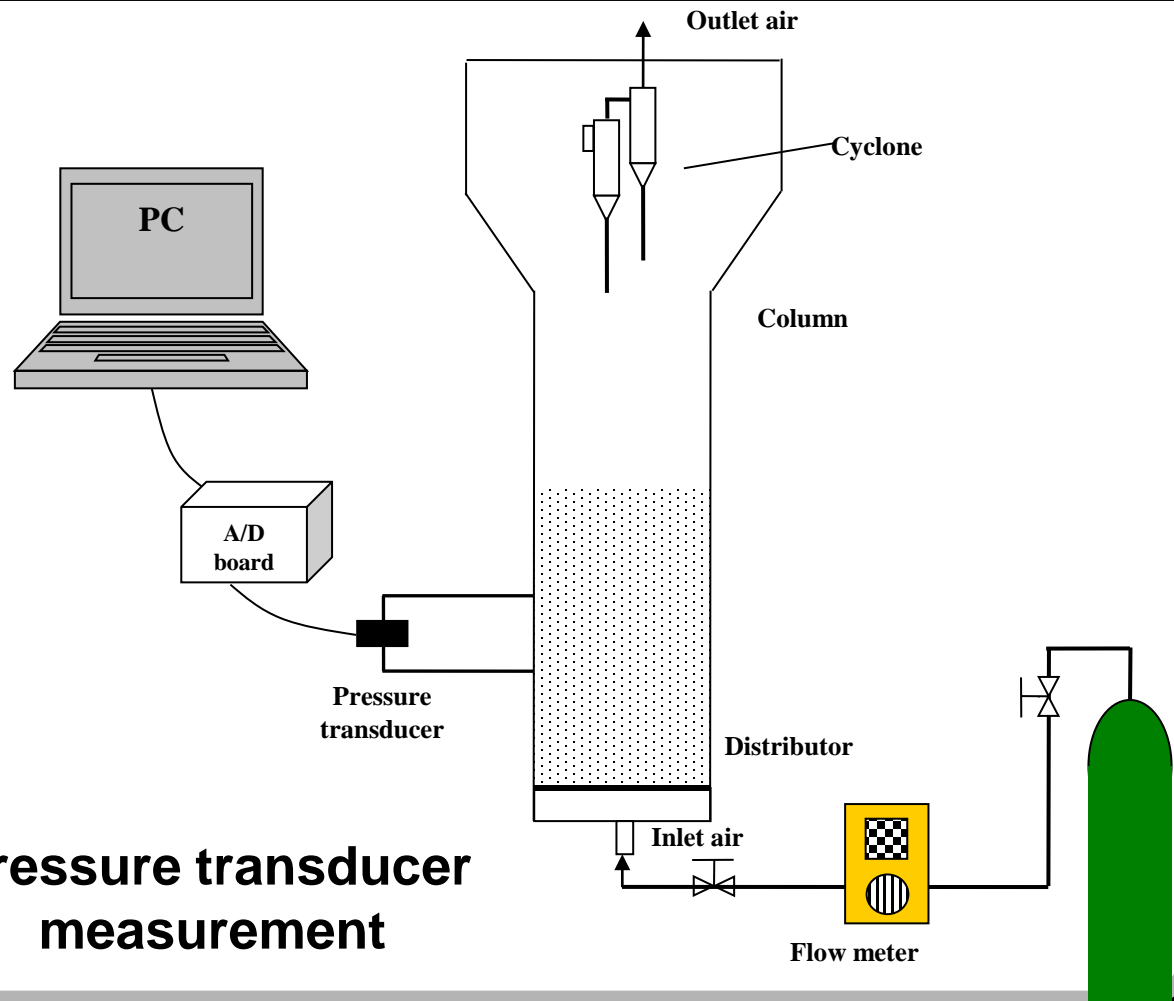
Flow meter

Gas Source

## Optical fiber probe measurement



## Pressure transducer measurement



# Experimental Conditions

1

## FCC particle:

Particle size: 60  $\mu\text{m}$

Particle density: 1400  $\text{kg/m}^3$

## Fluidized bed:

ID: 4 inch

Total height: 2.5 m

Two-stage cyclone

## Distributor:

Porous plate with a pore size of 20  $\mu\text{m}$

Fractional free area: 60%

## Gas:

Air density: 1.225  $\text{kg/m}^3$

Air viscosity:  $1.8 \times 10^{-5}$   $\text{Ns/m}^2$

2

## FCC particle:

Particle size: 60  $\mu\text{m}$

Particle density: 1400  $\text{kg/m}^3$

## Fluidized bed:

ID: 12 inch

Disengagement section: 0.5 m

Total height: 2.3 m

Two-stage cyclone

## Distributor:

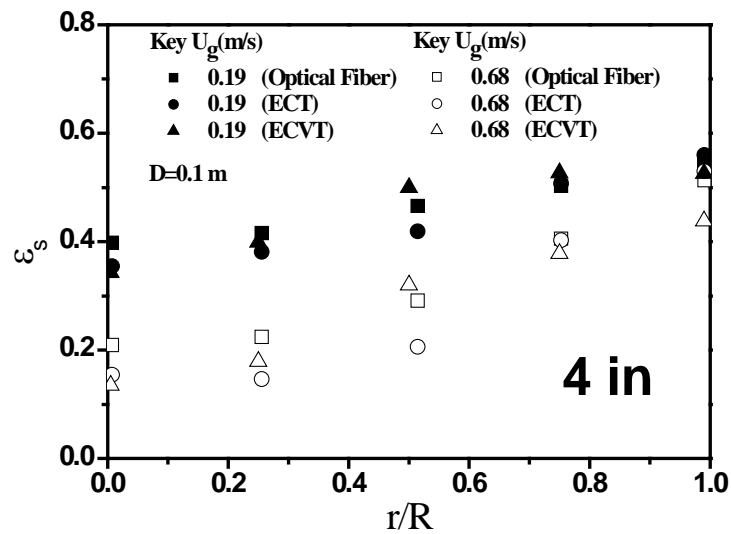
Porous plate with a pore size of 20  $\mu\text{m}$

Fractional free area: 60%

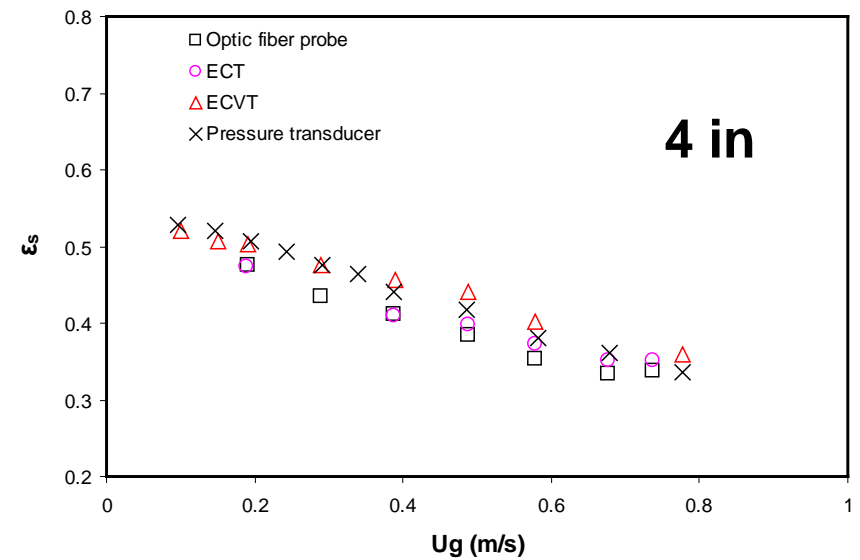
## Gas:

Air density: 1.225  $\text{kg/m}^3$

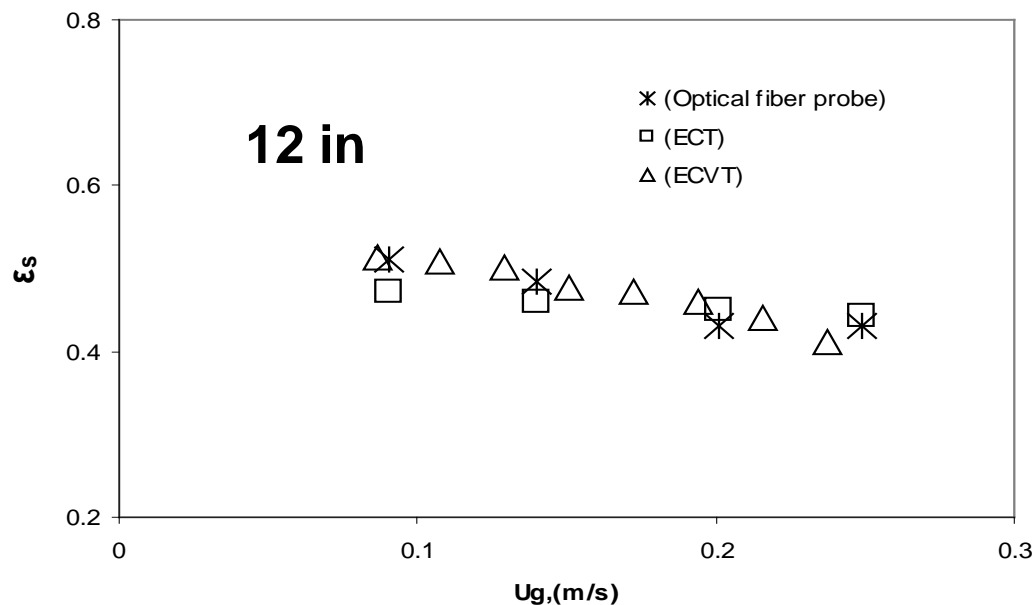
Air viscosity:  $1.8 \times 10^{-5}$   $\text{Ns/m}^2$



Radial profiles of time-averaged solids concentration in a 4-in gas-solid fluidized bed with FCC particles ( $d_p = 60 \mu\text{m}$ ;  $\rho_p = 1400 \text{ kg/m}^3$ ) obtained by ECVT, ECT and optical fiber probe

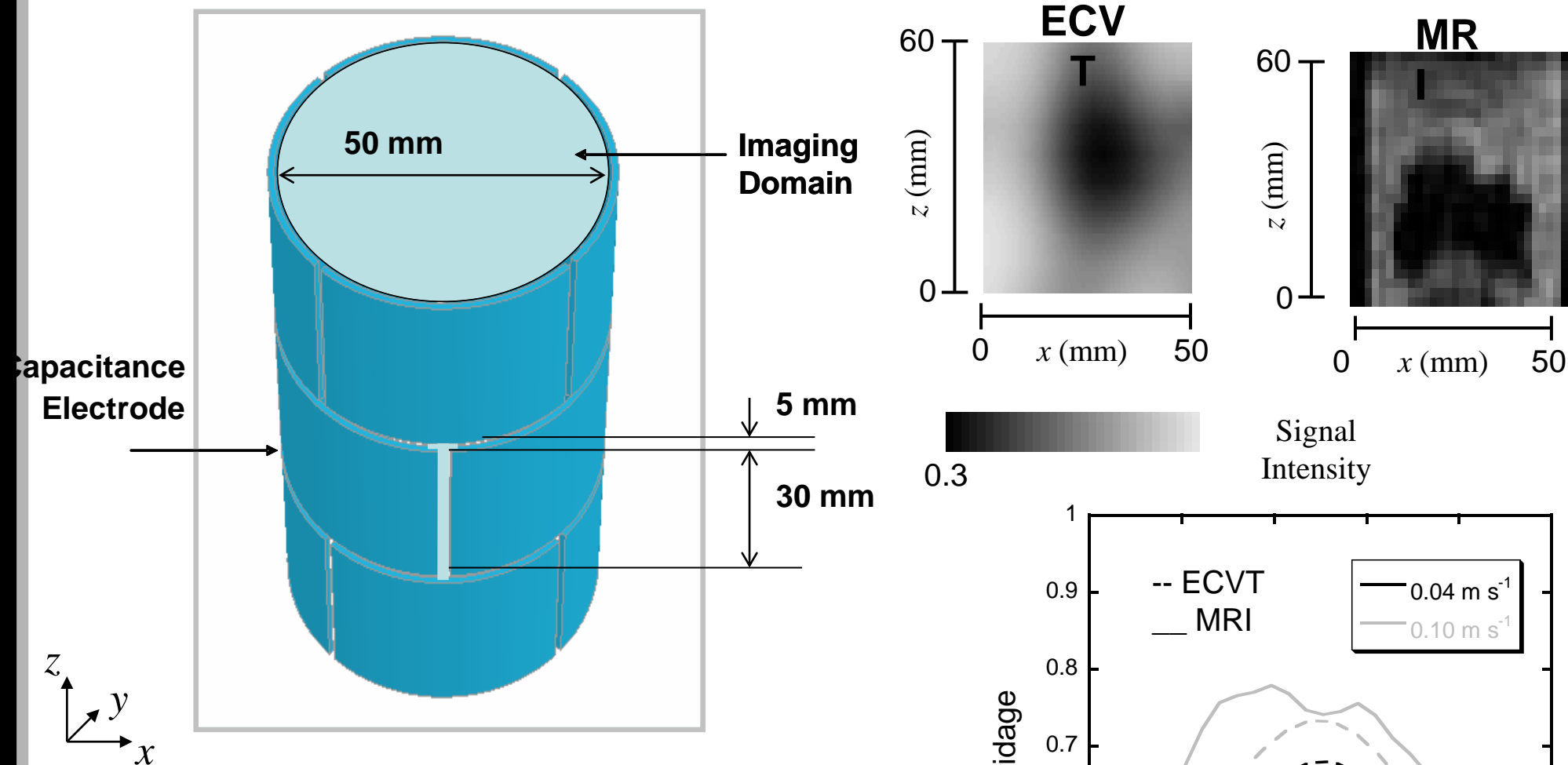


Comparison of the time-averaged cross-sectional solids concentrations obtained by ECT and optical fiber probe and the time-averaged volume solids concentration obtained by ECVT and pressure transducer for a 4-in gas-solid fluidized bed with FCC particles ( $d_p = 60 \mu\text{m}$ ;  $\rho_p = 1400 \text{ kg/m}^3$ )



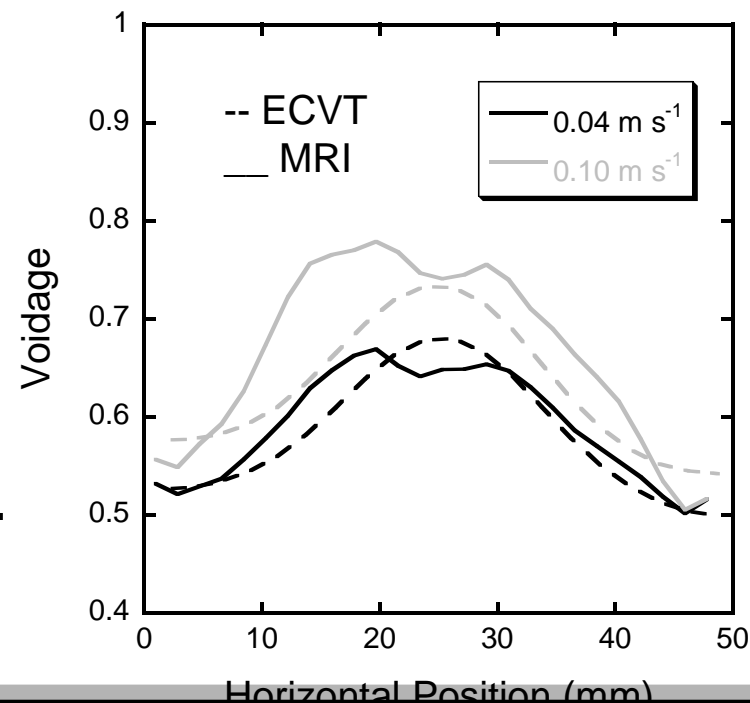
Comparison of the time-averaged cross-sectional solids concentrations obtained by the ECT and the optical fiber probe and the time-averaged volume solids concentration obtained by the ECVT for a 12-in gas-solid fluidized bed with FCC particles ( $d_p = 60 \mu\text{m}$ ;  $\rho_p = 1400 \text{ kg/m}^3$ )

# Electrical Capacitance Volume Tomography – Comparison with MRI

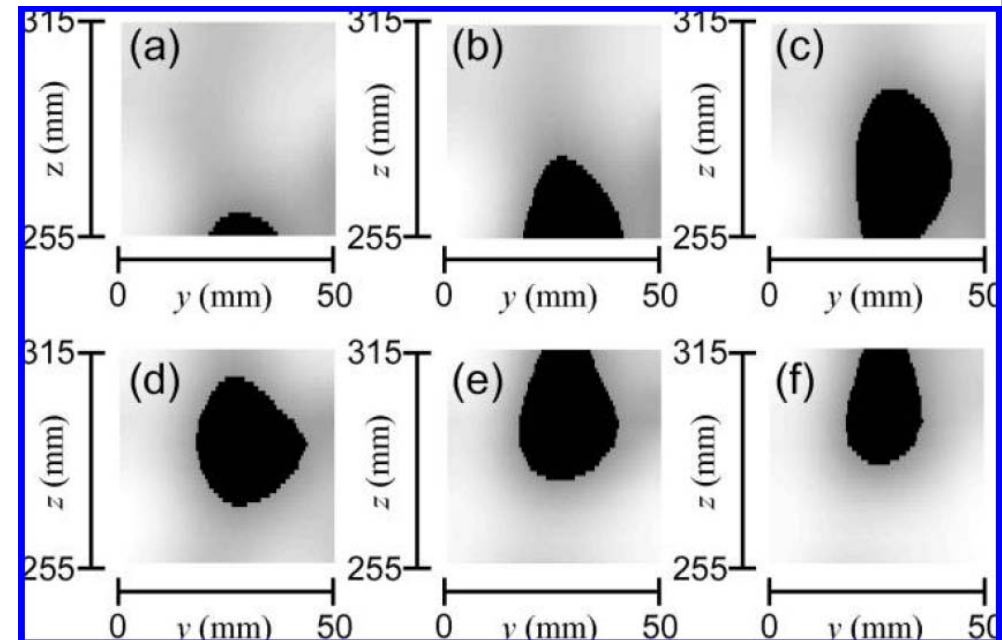
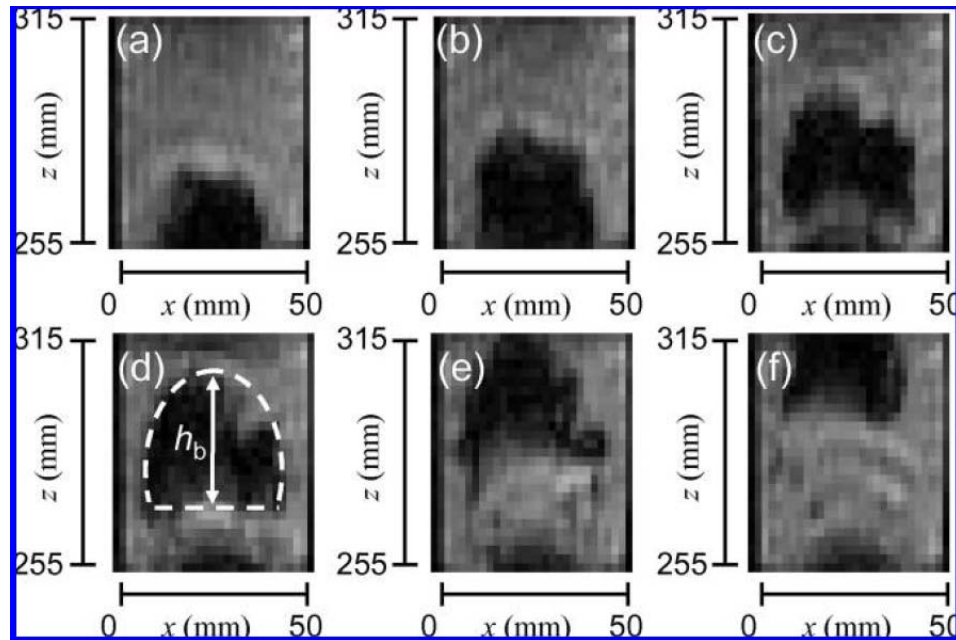


Work of **D.J. Holland<sup>1</sup>**, **Q. Marashdeh<sup>2</sup>**, **C.R. Müller<sup>1</sup>**, **F. Wang<sup>2</sup>**, **J.S. Dennis<sup>1</sup>**, **L.-S. Fan<sup>2</sup>**, **L.F. Gladden<sup>1</sup>**

<sup>1</sup>Cambridge University, <sup>2</sup>The Ohio State University



# Electrical Capacitance Volume Tomography – Comparison with MRI

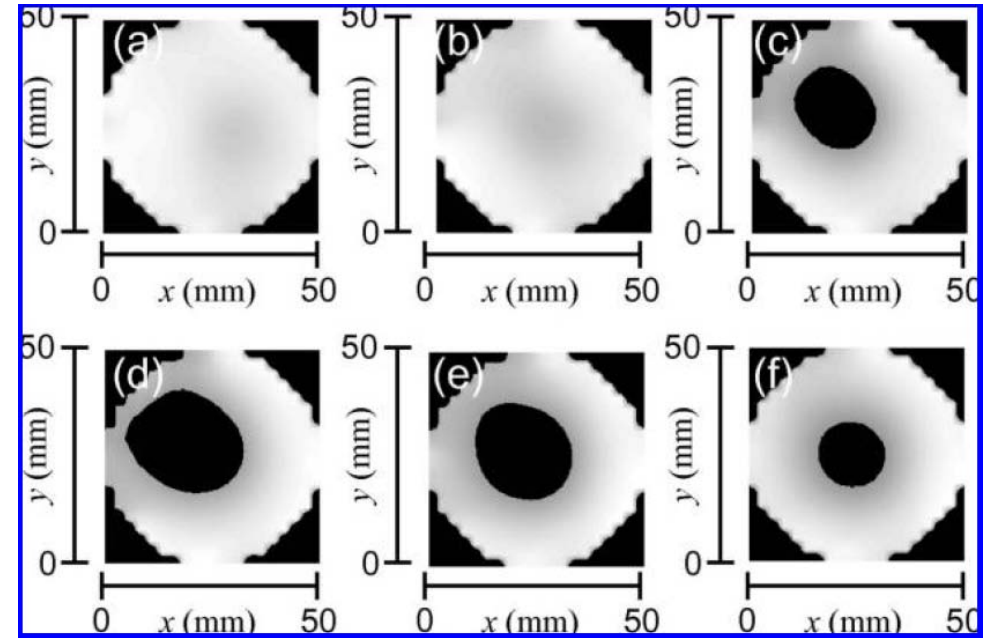
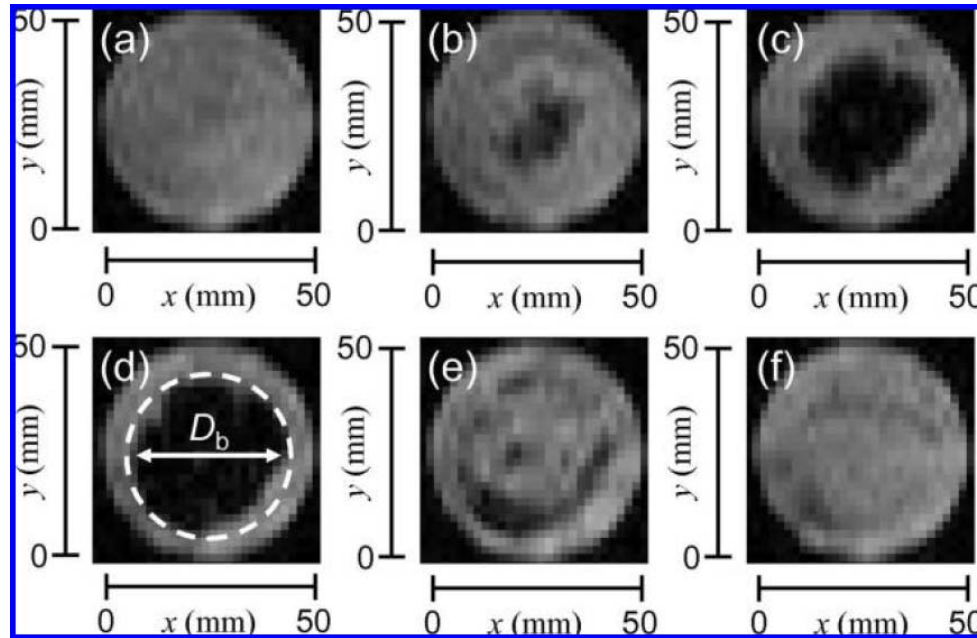


**Superficial Gas Velocity: 0.04 m/s;**  
**MRI: every frame (26 ms)**  
**ECVT: every 2<sup>nd</sup> frame (25 ms)**

Work of **D.J. Holland<sup>1</sup>**, **Q. Marashdeh<sup>2</sup>**, **C.R. Müller<sup>1</sup>**, **F. Wang<sup>2</sup>**, **J.S. Dennis<sup>1</sup>**,  
**L.-S. Fan<sup>2</sup>**, **L.F. Gladden<sup>1</sup>**

<sup>1</sup>Cambridge University, <sup>2</sup>The Ohio State University

# Electrical Capacitance Volume Tomography – Comparison with MRI

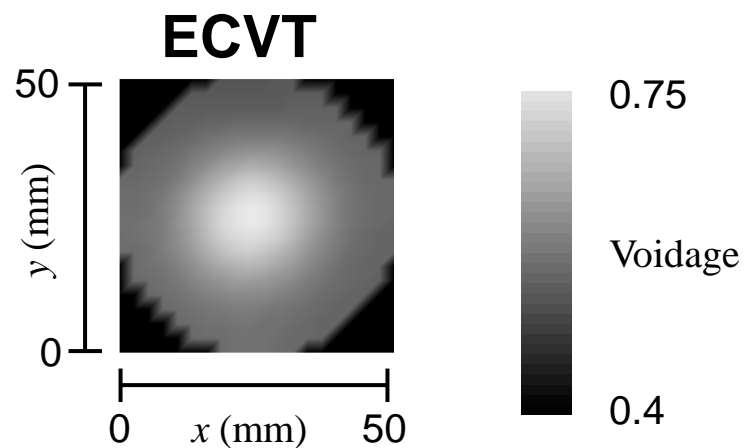
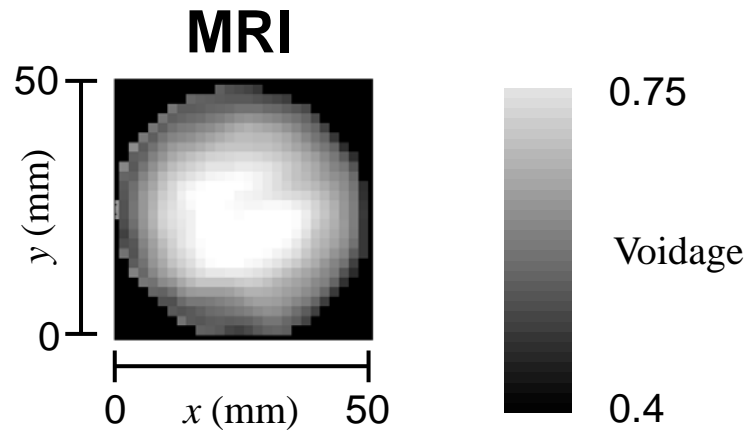


**Superficial Gas Velocity: 0.04 m/s;**  
**MRI: every frame (26 ms)**  
**ECVT: every 2<sup>nd</sup> frame (25 ms)**

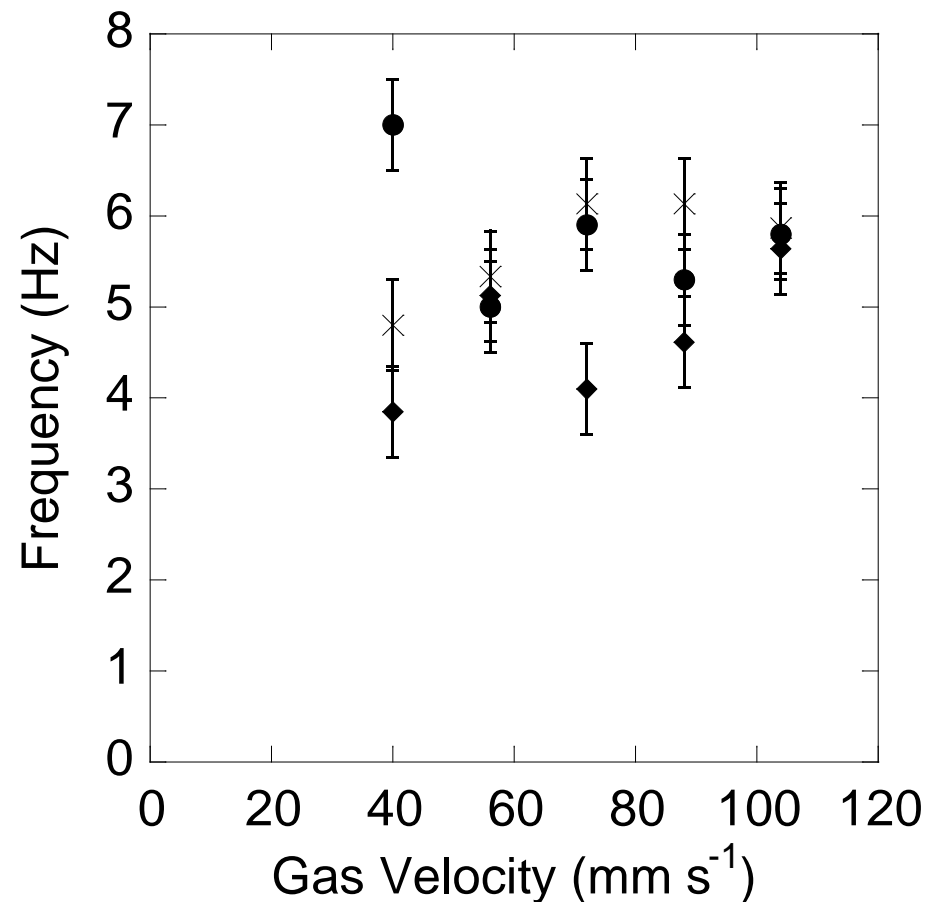
Work of **D.J. Holland<sup>1</sup>**, **Q. Marashdeh<sup>2</sup>**, **C.R. Müller<sup>1</sup>**, **F. Wang<sup>2</sup>**, **J.S. Dennis<sup>1</sup>**,  
**L.-S. Fan<sup>2</sup>**, **L.F. Gladden<sup>1</sup>**

<sup>1</sup>Cambridge University, <sup>2</sup>The Ohio State University

# Electrical Capacitance Volume Tomography – Comparison with MRI



**Superficial Gas Velocity:  
0.104 m s<sup>-1</sup>**



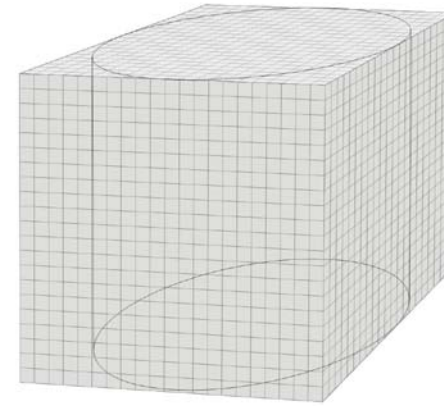
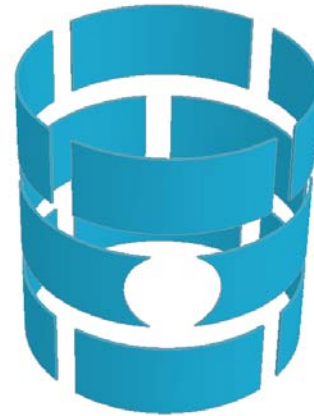
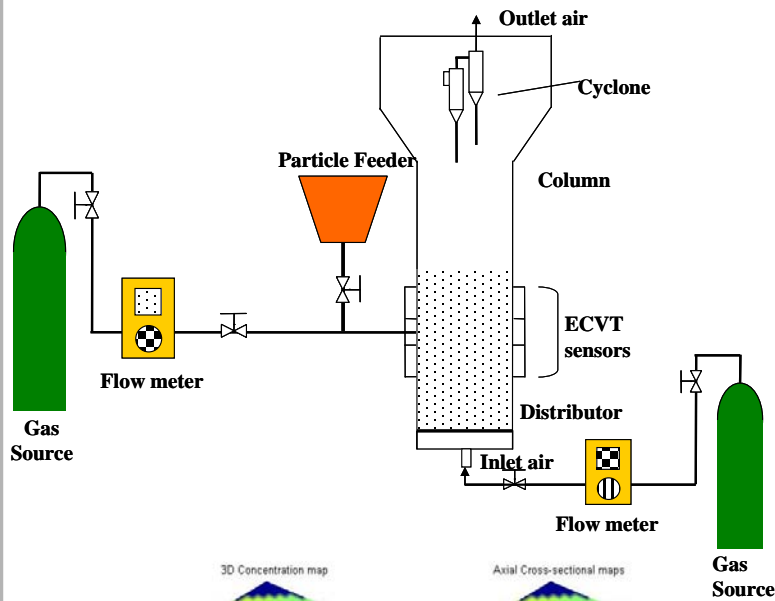
**Bubble frequency calculated from  
the ECVT (×), 2D MR data (◆) and 1D  
MR data (●).**

Work of D.J. Holland<sup>1</sup>, Q. Marashdeh<sup>2</sup>, C.R. Müller<sup>1</sup>, F.  
Wang<sup>2</sup>, J.S. Dennis<sup>1</sup>, L.-S. Fan<sup>2</sup>, L.F. Gladden<sup>1</sup>

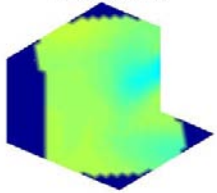
<sup>1</sup>Cambridge University, <sup>2</sup>The Ohio State University



# 3. Horizontal gas jet penetration in a gas-solid fluidized bed



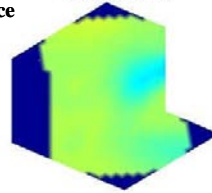
3D Concentration map



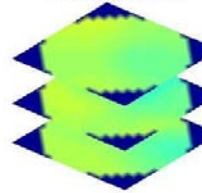
Axial Cross-sectional maps



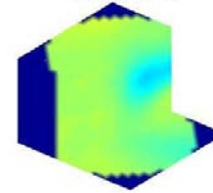
3D Concentration map



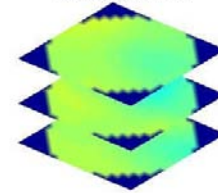
Axial Cross-sectional maps



3D Concentration map

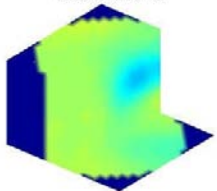


Axial Cross-sectional maps



(a)  $t=0$ ; (b)  $t=12.5$  ms; (c)  $t=25.0$  ms; (d)  $t=37.5$ ; (e)  $t=50.0$  ms; (f)  $t=62.5$  ms.  $U_g=0.064$  m/s,  $U_0=15$  m/s

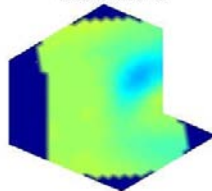
3D Concentration map



Axial Cross-sectional maps



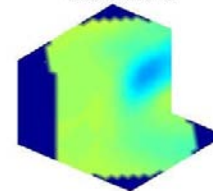
3D Concentration map



Axial Cross-sectional maps



3D Concentration map



Axial Cross-sectional maps



Dynamic  
Of  
Jet  
Penetration

# Experimental Conditions

## FCC particle:

Particle size: 60  $\mu\text{m}$

Particle density: 1400  $\text{kg/m}^3$

## Fluidized bed:

ID: 12 inch

Disengagement section: 0.5 m

Total height: 2.3 m

Two-stage cyclone

## Distributor:

Porous plate with a pore size of 20  $\mu\text{m}$

Fractional free area: 60%

## Gas:

Air density: 1.225  $\text{kg/m}^3$

Air viscosity:  $1.8 \times 10^{-5}$   $\text{Ns/m}^2$

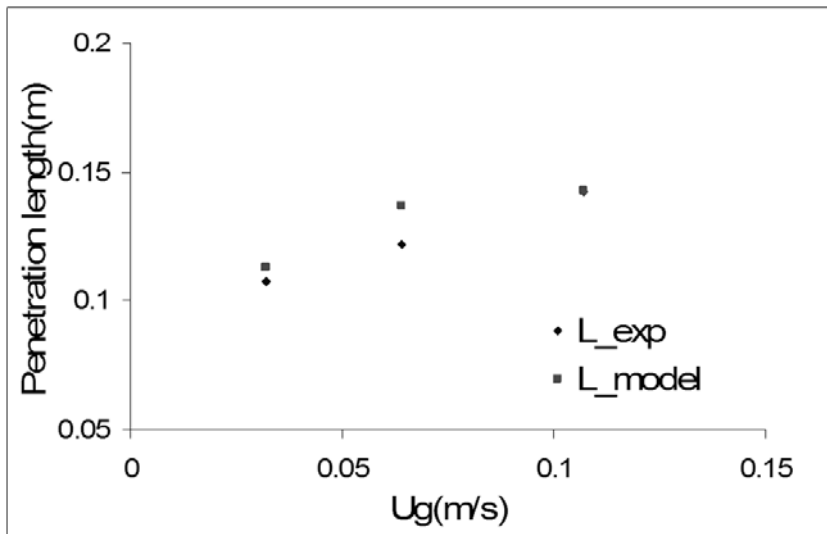
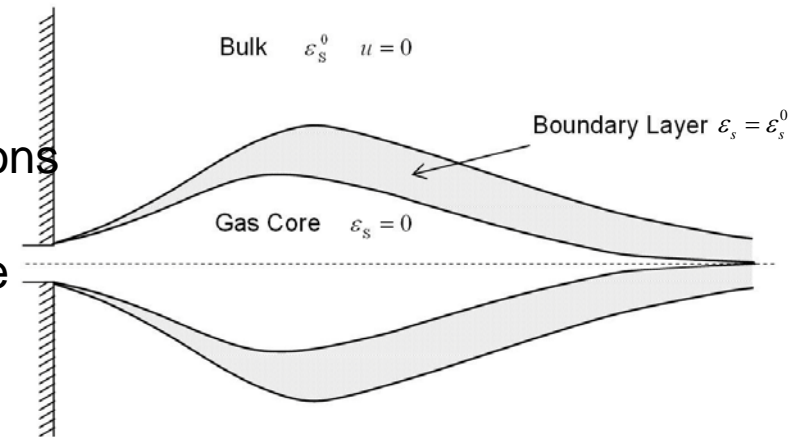
# Sensors and Experimental Setup



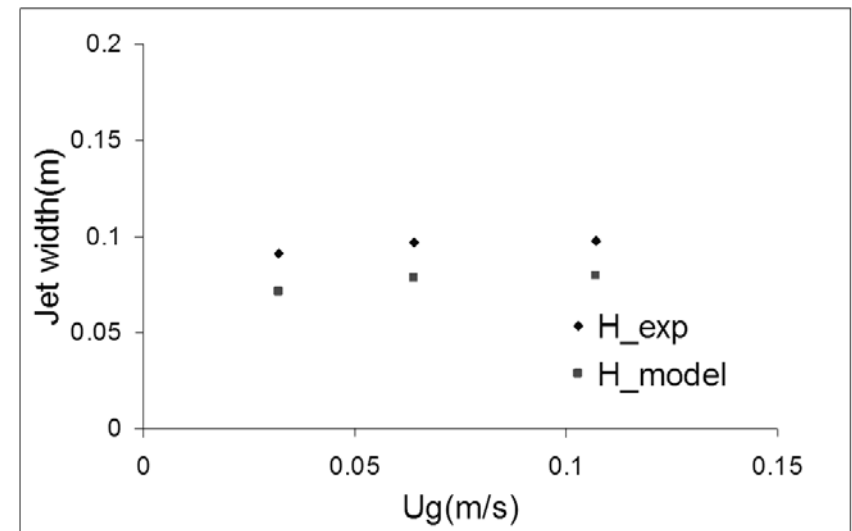
# Horizontal gas jet penetration in a gas-solid fluidized bed

## Horizontal jet in a gas-solid fluidized bed:

- solid particle holdup varies in the radial and axial directions
- particles entrain into the jet
- momentum is transferred from the jet to the solid particle
- the closure of the jet is due to the momentum loss



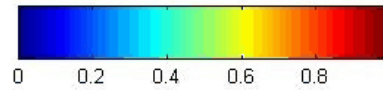
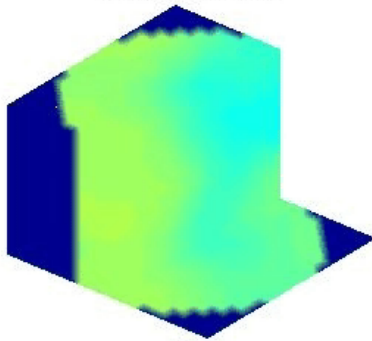
Comparison of the maximum penetration lengths of the horizontal gas jet obtained by ECVT experiments and model prediction for the 0.3 m gas-solid fluidized bed



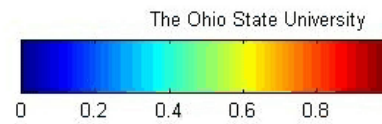
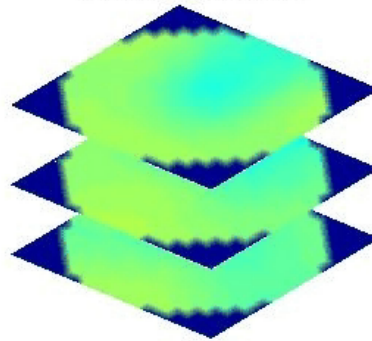
Comparison of the maximum width of the horizontal gas jet obtained by ECVT experiments and model prediction for the 0.3 m gas-solid fluidized bed



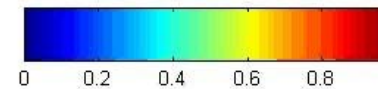
3D Concentration map



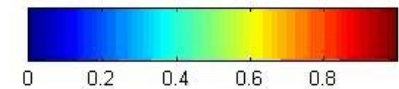
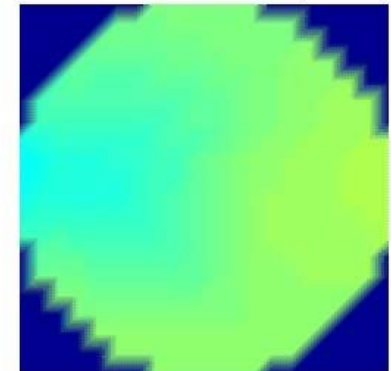
Axial Cross-sectional maps



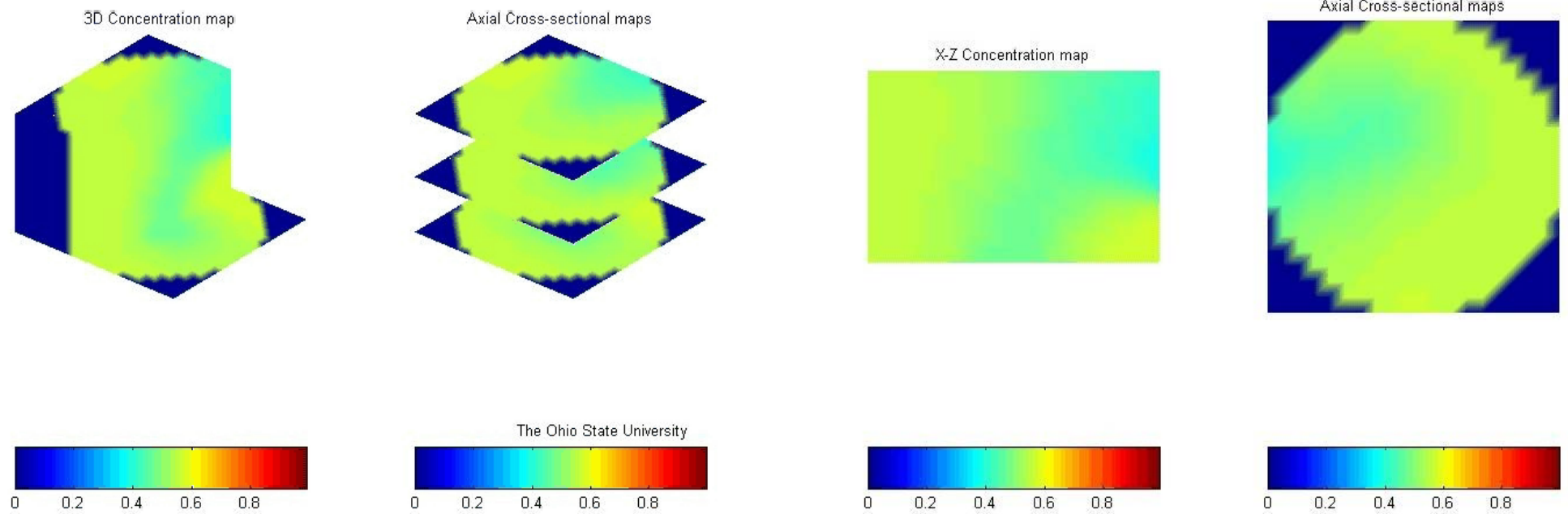
X-Z Concentration map



Axial Cross-sectional maps

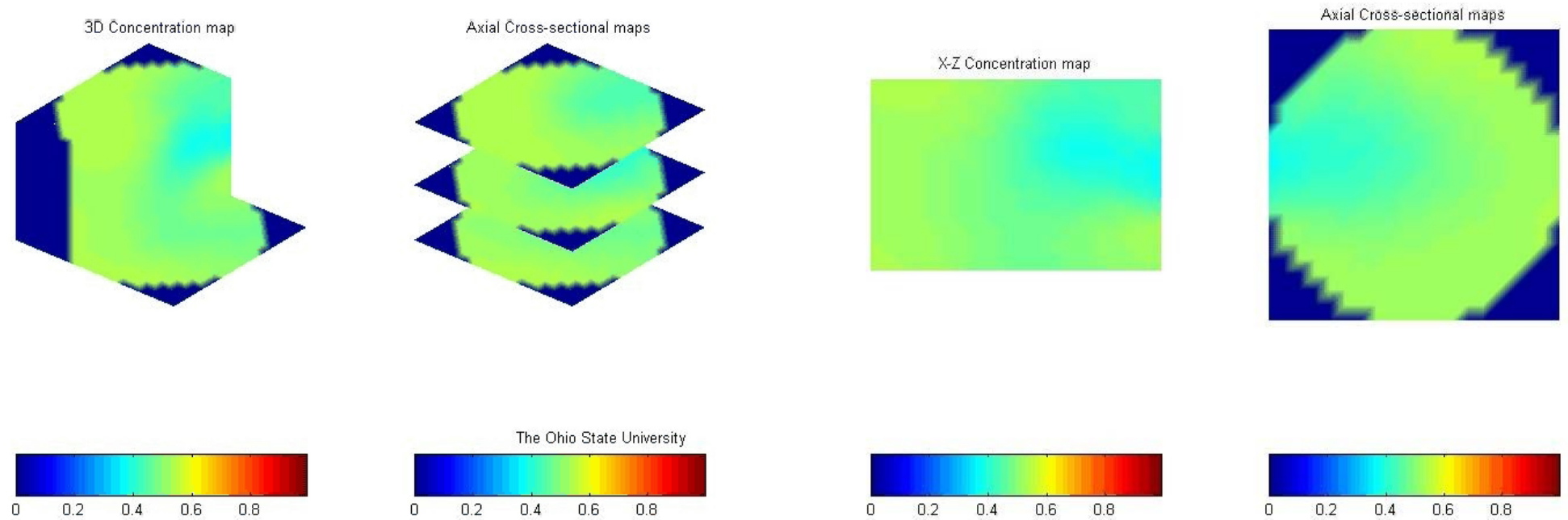


Superficial gas velocity:  $U_g = 0.108$  m/s  
 Side gas velocity:  $U_{g\_side} = 15.5$  m/s  
 Side solids velocity:  $U_{s\_side} = 0$



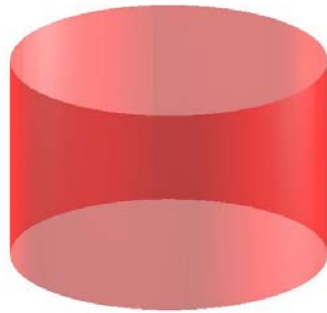
Superficial gas velocity:  $U_g=0.032$  m/s; Side gas velocity:  $U_{g\_side}=15.5$  m/s; Side solids velocity:  $U_{s\_side}=0$

Superficial gas velocity:  $U_g=0.032$  m/s; Side gas velocity:  $U_{g\_side}=16.3$  m/s; Side solids velocity:  $U_{s\_side}=16.3$  m/s

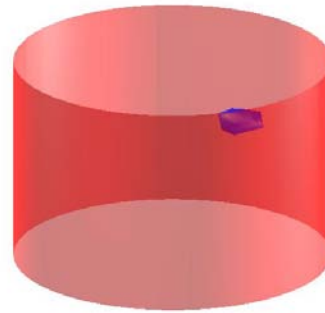


# Jet shape from ECVT images

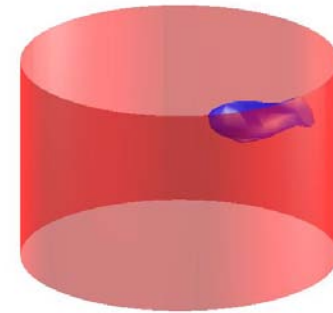
(Maximum jet penetration)



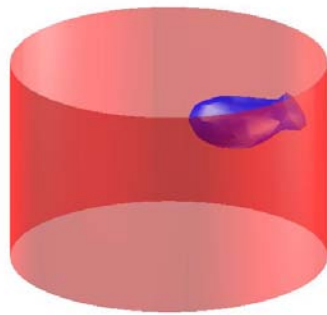
$t=0$



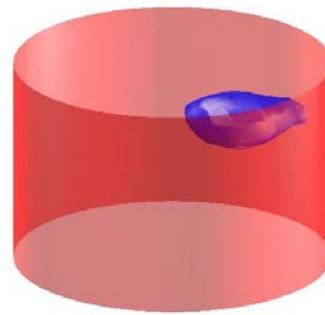
$t=12.5$  ms



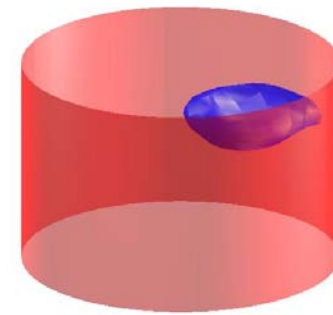
$t=25$  ms



$t=37.5$  ms



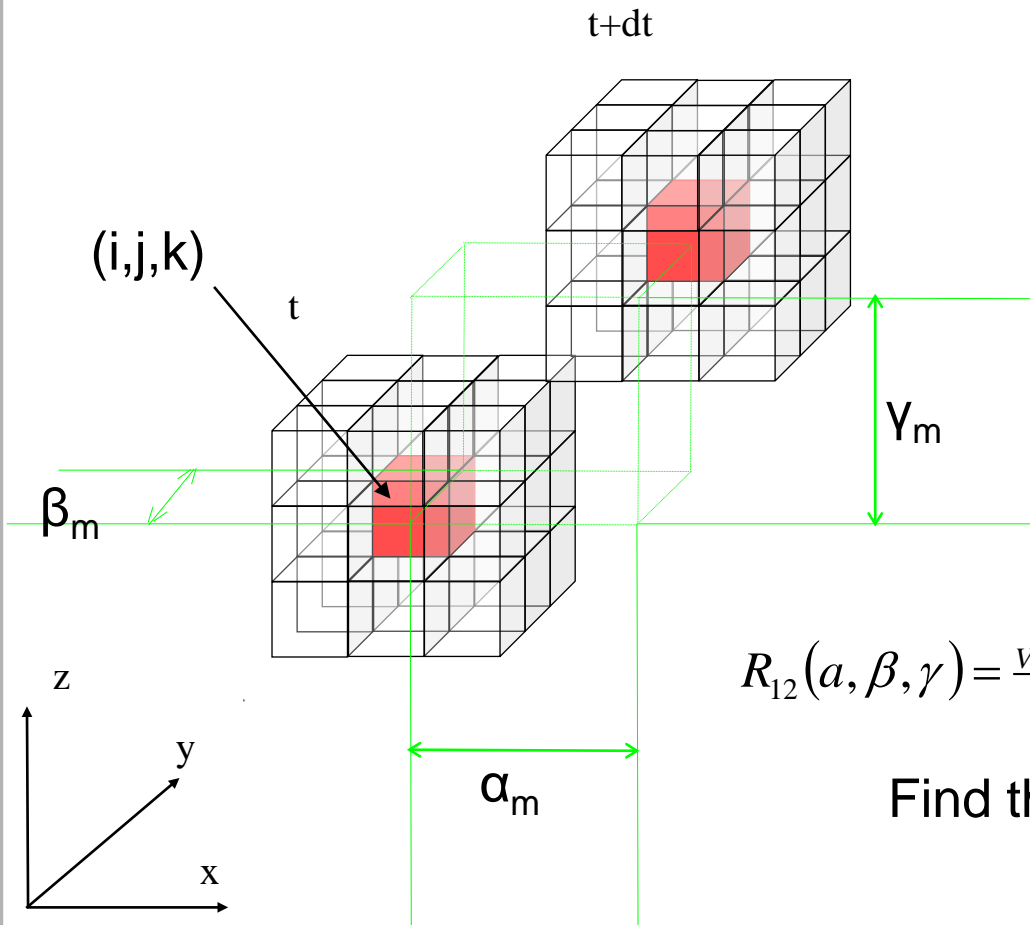
$t=50$  ms



$t=62.5$  ms

$U_g=0.064$  m/s,  $U_0=15$   
m/s

# 4. Velocimetry



Choose a window

At Voxel  $(i,j,k)$ :

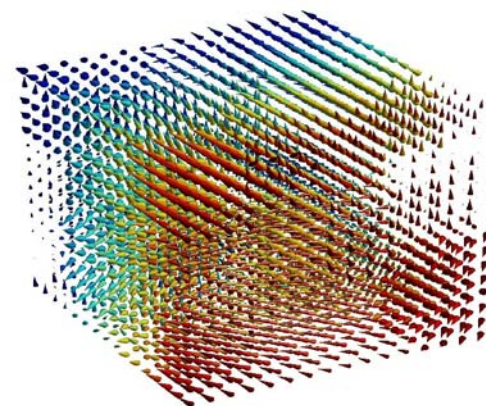
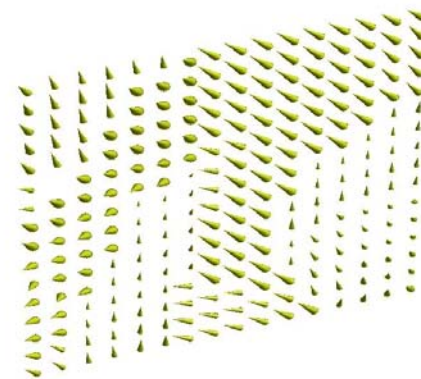
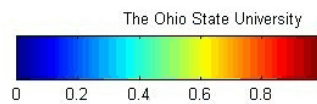
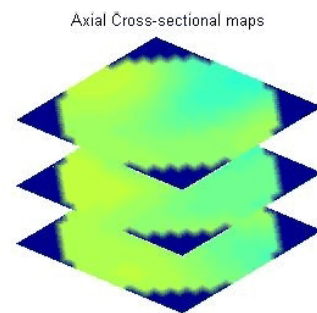
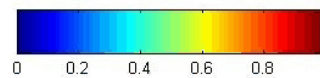
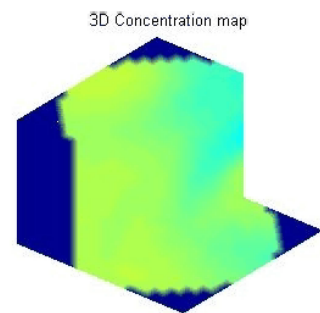
$$R_{12}(a, \beta, \gamma) = \frac{\int_{V\text{-Window}} V_1(x, y, z, t) V_2(x + \alpha, y + \beta, z + \gamma, t + \Delta t) dx dy dz}{|V_1| \cdot |V_2|}$$

Find the maximum  $R_{12}$  at  $(\alpha_m, \beta_m, \gamma_m)$

Voxel volume averaged phase velocity at Voxel  $(i,j,k)$ :

$$v_x = \frac{\alpha_m - i}{\Delta t} \Delta x \quad v_y = \frac{\beta_m - j}{\Delta t} \Delta y \quad v_z = \frac{\gamma_m - k}{\Delta t} \Delta z$$

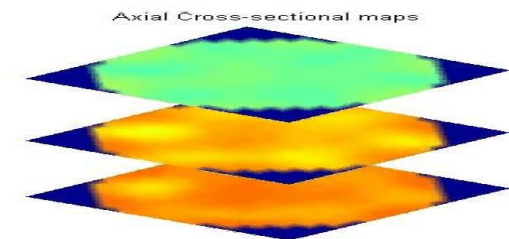
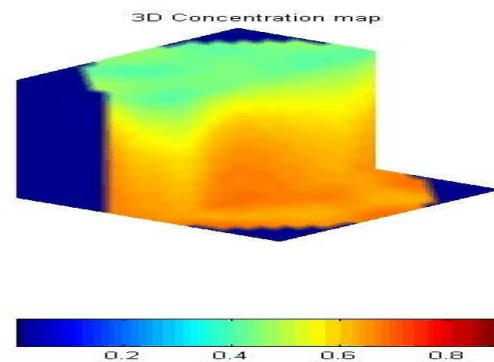
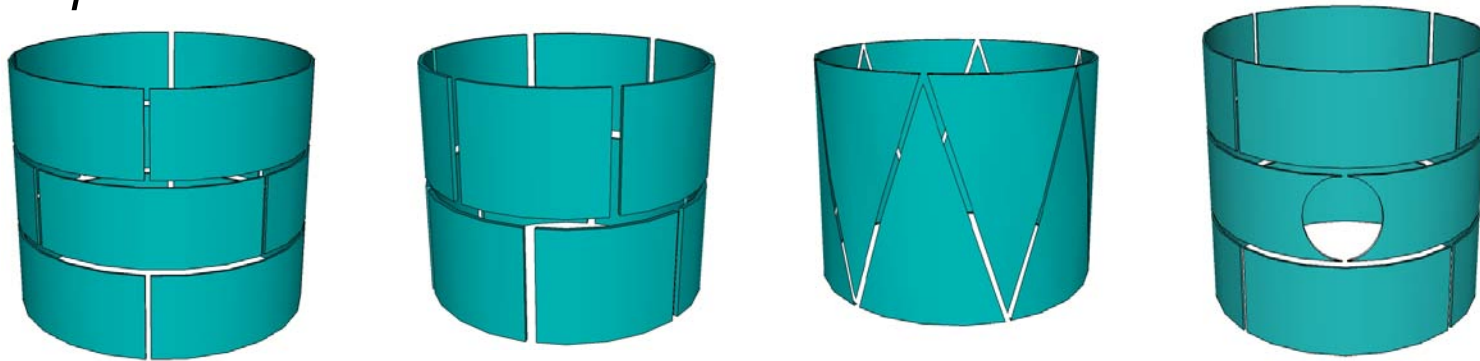




$U_g = 0.064 \text{ m/s}$ ,  $U_0 = 15 \text{ m/s}$

# 5. ECVT Sensor Applications

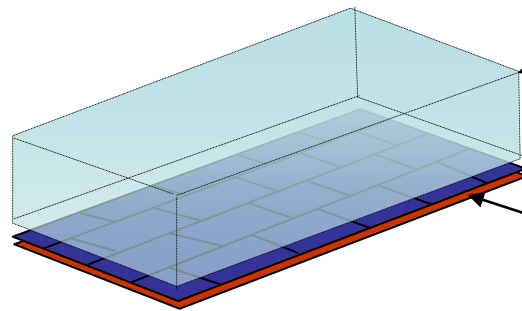
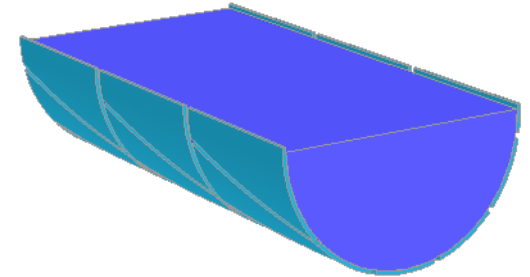
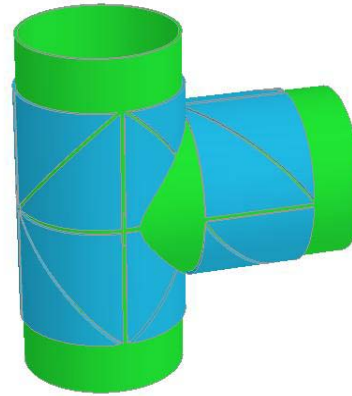
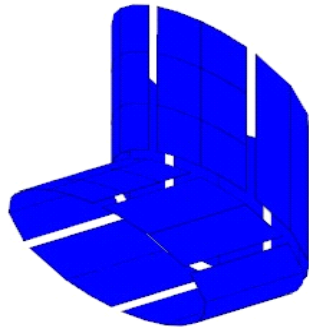
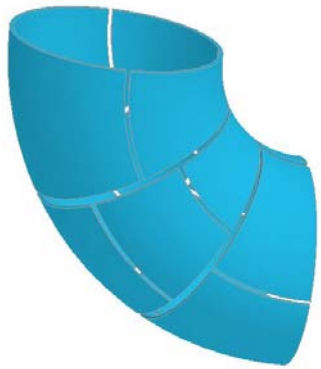
*Cylindrical shape sensor*



SCR12-25

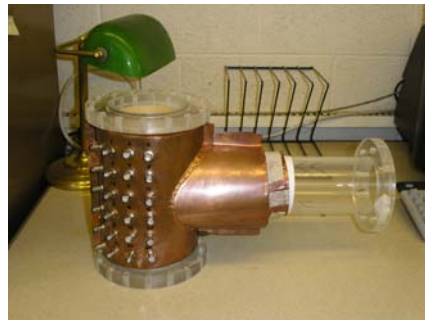
# ECVT sensor design

*Sensors with complex geometries*



Sensing  
domain  
voxels

Planar sensor  
electrodes



# ECVT sensor design

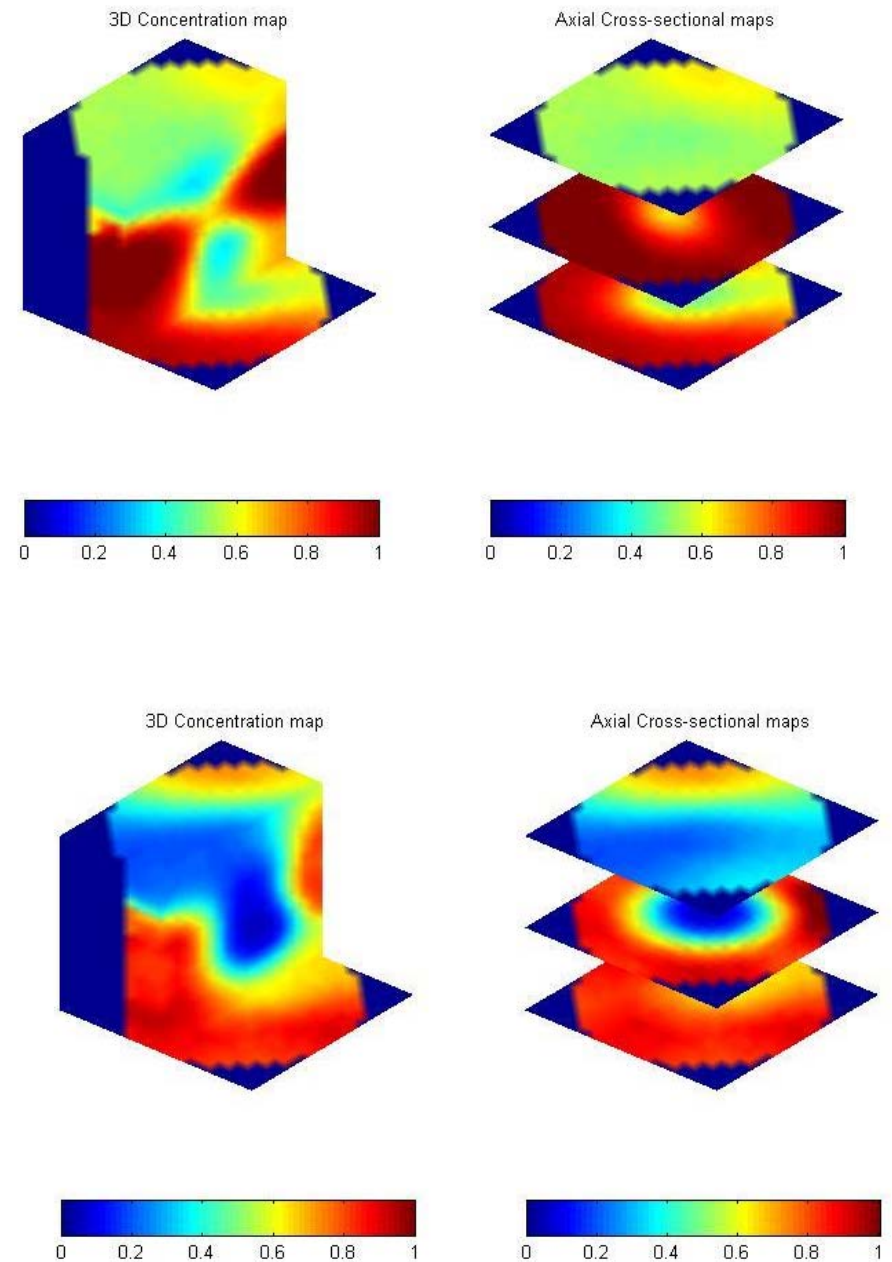
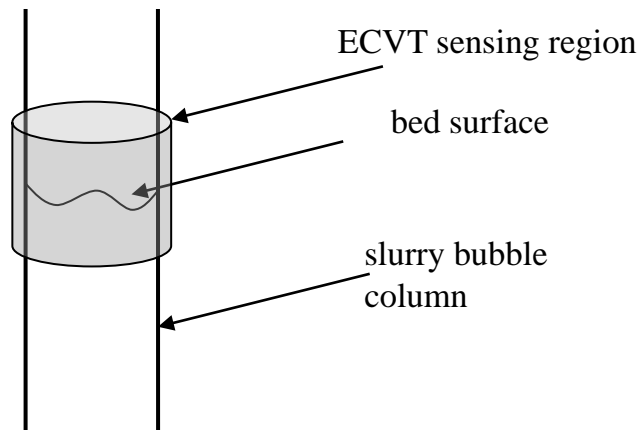
**Comparison of different sensor geometries in terms of symmetry, axial resolution and radial resolution**

Sensor Type	Sensor Symmetry	Axial Resolution	Radial Resolution
<b>Cylindrical sensor with 1 layer</b>	High	Low, sensitivity decreases toward center.	High, sensitivity decreases toward center.
<b>Cylindrical sensor with 2 shifted layers</b>	Moderate	Moderate, sensitivity decreases toward center.	Moderate, sensitivity decreases toward center
<b>Cylindrical sensor with 3 shifted layers</b>	Moderate	High, sensitivity decreases toward center.	Moderate-High, sensitivity decreases toward center.
<b>Planar sensor with shifted planes</b>	Moderate	Low, sensitivity decreases away from sensor.	High, Sensitivity decreases away from sensor.
<b>Bent sensor</b>	Low	Depends on sensor plate arrangement	Depends on sensor plates arrangement

Fei Wang, Qussai Marashdeh, Liang-Shih Fan \* and Warsito Warsito “Electrical Capacitance Volume Tomography: Design and Applications” *Sensors* **2010**, *10*, 1890-1917;



# Surface of Slurry Bubble Columns

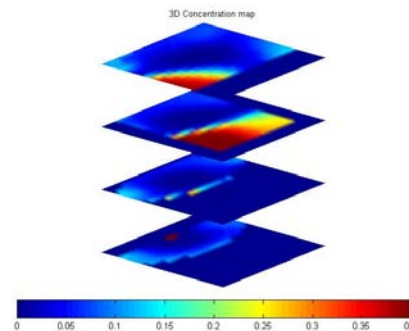
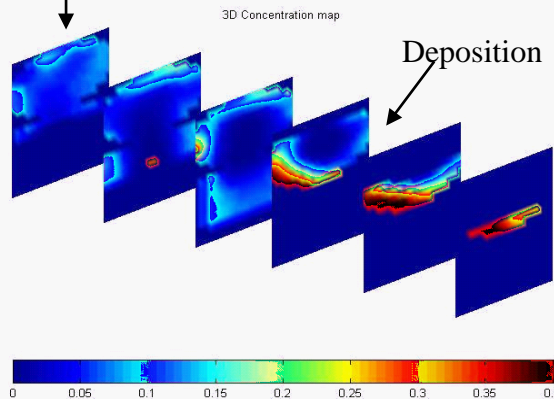
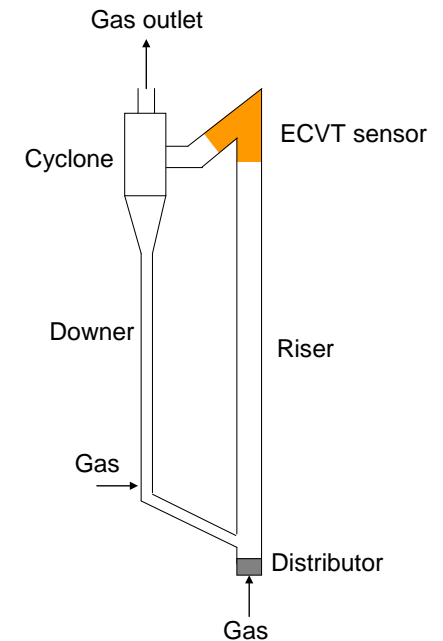
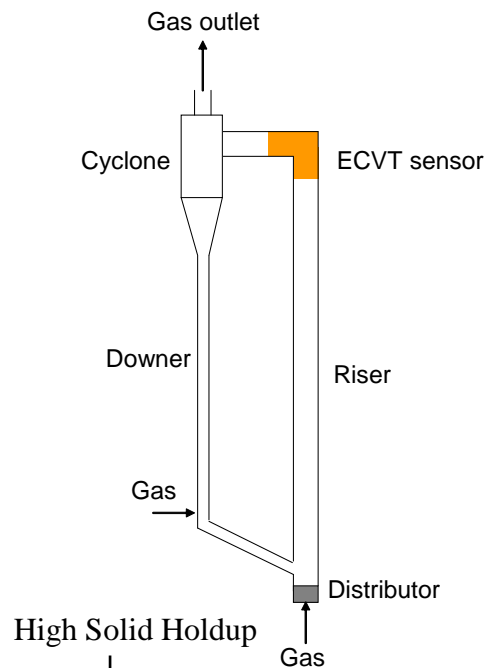


Snapshots of bubble bursting at the surface of a slurry bubble column by ECVT:  
(a) 3D image before bubble bursting; (b) 3D image after bubble bursting

## 6. Complex Geometries Examples

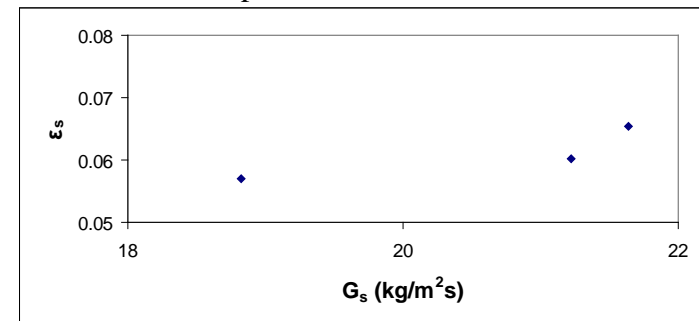


# 3-D gas-solid flow patterns in the exit region of a gas-solid CFB riser

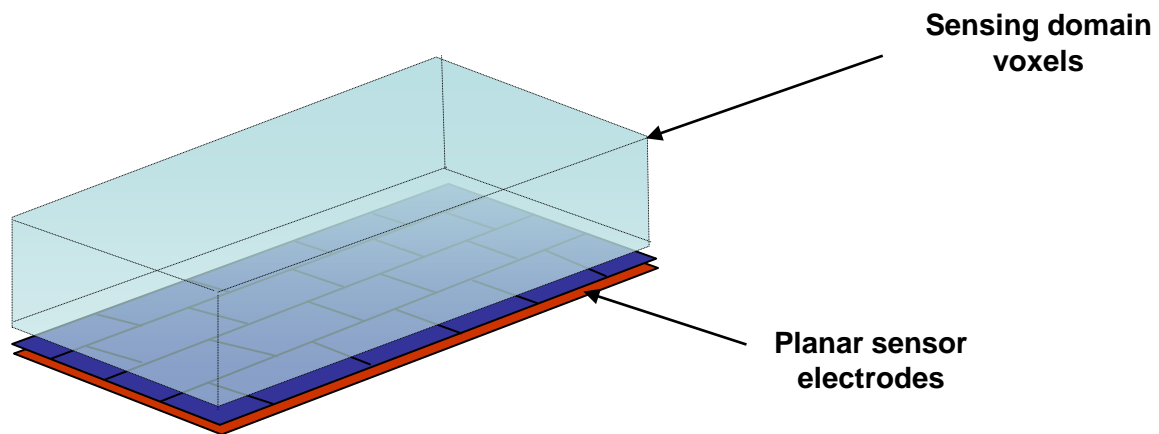


Solids holdup distribution in the bend of the CFB riser at  $U_g=1.36$  m/s and  $G_s=21.2$  kg/m<sup>2</sup>s: vertical slices and horizontal slices

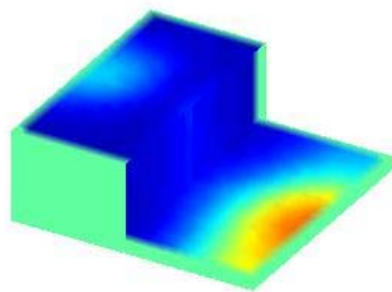
Solids Holdup/ Solid Circulation Rate



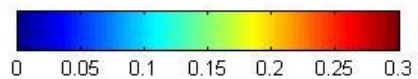
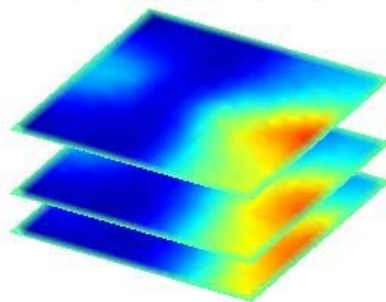
Time-averaged volume solids holdup at the top wall region at the start of the horizontal duct of the bend at  $U_g=1.16$  m/s



3D Concentration map



Axial Cross-sectional maps



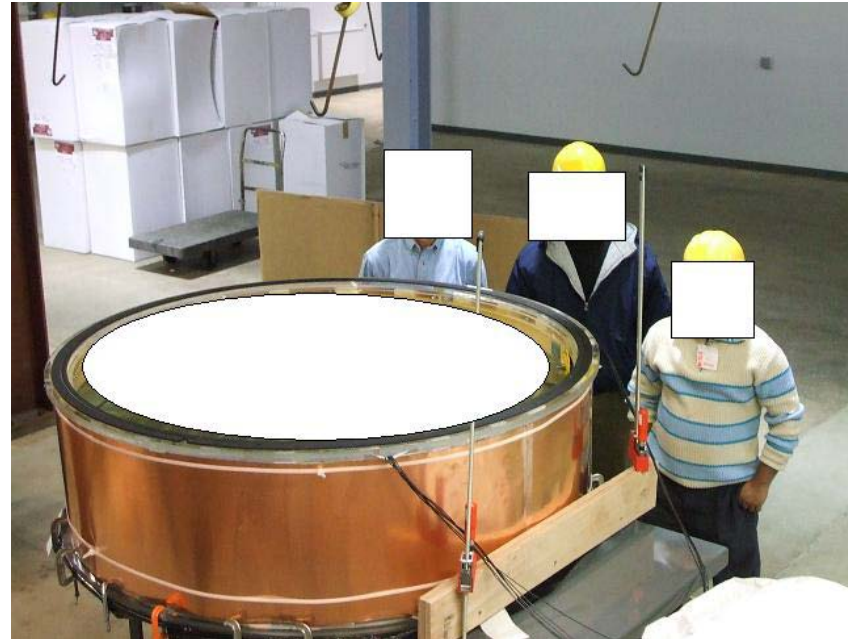


# Scale-Up ECVT Sensors

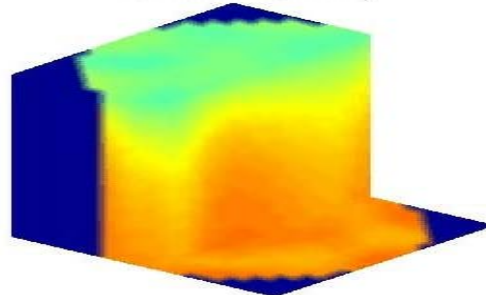


60 inch ID →

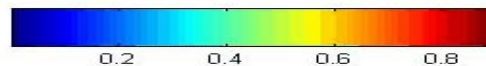
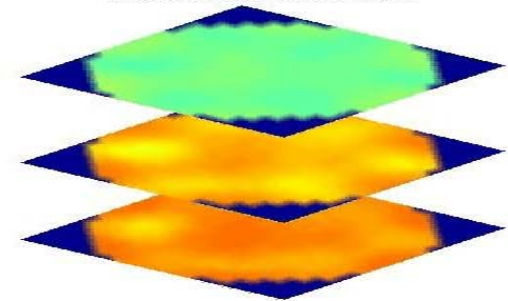
← 12 inch ID



3D Concentration map



Axial Cross-sectional maps



# Concluding Remarks

- ◆ ECVT is a non-invasive imaging technology that can be applied to image processes vessels of various diameters.
- ◆ ECVT is a unique imaging technology with its potential for commercial scale-up
- ◆ Tech4Imaging LLC is developing a commercial ECVT system for imaging multi-phase flow systems.

# Acknowledgement

- ◆ The support of US. Department of Energy under Grant # DE-NT0006564 is gratefully acknowledged
- ◆ Dr. W. Warsito, Dr. Bing Du, Dr. Zhao Yu, and all students who worked or are working on ECVT technology are also acknowledged.

